Catalysis Today 383 (2022) 123–132

Contents lists available at ScienceDirect

Catalysis Today

journal homepage: www.elsevier.com/locate/cattod

Rich H_2 catalytic oxidation as a novel methodology for the evaluation of mass transport properties of 3D printed catalyst supports

Federico Sascha Franchi, Matteo Ambrosetti, Riccardo Balzarotti, Mauro Bracconi, Gianpiero Groppi *, Enrico Tronconi

Politecnico di Milano, Dipartimento di Energia, Via Lambruschini 4, 20156, Milano, Italy

ARTICLE INFO

Keywords:
Mass transfer
3D printing
Structured catalysts
POCS
H_2 oxidation

ABSTRACT

In this work, we propose a novel methodology for the evaluation of the external mass transfer properties of 3D printed catalyst supports. This protocol relies on the use of a lab scale SLA 3D printer with a resin characterized by a high heat deflection temperature (HDT) for the manufacturing of samples at a lower price and with higher accuracy than equivalent metallic 3D printed structures. Periodic open cellular structure (POCS) samples with Tetrakaidecahedron unit cells (TKKD) were 3D printed and catalytically activated by depositing a 3% Pd/CeO_2 washcoat by spin-coating. The washcoat was then consolidated with a two-step heat treatment composed by in-situ calcination in N_2 and reduction in N_2/H_2 stream. Catalytic tests of rich H_2 combustion showed the possibility to reach the external mass transfer control at temperatures below the resin HDT. Sherwood numbers were eventually estimated from the oxygen conversions under full external mass transfer control assuming a PFR behaviour. To validate the methodology, 3D printed replicas of open cell foams were also tested, and the results were successfully compared against a well-established literature correlation. Moreover, a one-to-one comparison was performed between the Sherwood numbers of a resin 3D printed structure, tested with the proposed methodology, and a metallic 3D printed structure, tested with the conventional CO oxidation approach. The two methods lead to superimposed results, thus providing the experimental evidence of the equivalence of the two methodologies for the evaluation of the external mass transport properties of complex catalyst substrates.

1. Introduction

To meet the current growing interest in the intensification of industrial and environmental heterogeneous catalytic processes, a wide range of advanced structures based on wire meshes, open cell foams and periodic open cellular structures (POCS) [1] are under study by the research community.

Open cell foams have been extensively investigated in the last decade as high performance supports for processes limited by gas/solid mass and/or heat transfer [2–8]. Differently from open cell foams, POCS have an ordered geometry and are generally manufactured by 3D printing techniques. In recent years, literature works have shown promising results of the application of these materials in processes where the optimal tradeoff between pressure drops [9] and mass transfer is crucial, such as exhaust gas after-treatment systems [10,11] or where heat transfer is the limiting factor for the application [12].

Thanks to the extreme design freedom provided by their manufacturing methodology, a great number of POCS with different geometries and dimensions can be realized and Computational Fluid Dynamics (CFD) can be a powerful tool for the numerical evaluation of their transport properties [10,13]. However, such a large design flexibility poses the problem of how an experimental screening can be performed for a wide range of different cell shapes and sizes in order to identify the most effective structures and to develop engineering correlations for the simple prediction of their behavior. To these aims, it was demonstrated that 3D printed structures produced with different materials may be employed for the evaluation of pressure drop [10,14] or for the heat transport [5]. However, the analysis of external mass transfer properties poses great challenges on the design of the experimental protocols and on the selection of the sample properties.

Abbreviations: CAD, computer-aided design; CeHS, high surface area CeO_2; CFD, computational fluid dynamics; GC, gas chromatographer; HDT, heat deflection temperature; HT, high temperature; IPA, isopropyl alcohol; Pd/CeHS, palladium on high surface area CeO_2; PGM, precious group metals; POCS, periodic open cellular structures; PVA, polyvinyl alcohol; SLA, stereolithography; SLM, selective laser melting; TCD, thermal conductivity detector; TKKD, tetrakaidekahedron.

* Corresponding author.
E-mail address: gianpiero.groppi@polimi.it (G. Groppi).

https://doi.org/10.1016/j.cattod.2021.04.004
Received 30 October 2020; Received in revised form 8 March 2021; Accepted 5 April 2021
Available online 9 April 2021

Several methodologies for the evaluation of the external mass transfer in cellular catalyst substrates have been reported in literature. Some of these methods are based on the dissolution/sublimation of a suitable substance coated on or with the shape of the required geometry. Yagi et al. [15] and Dixon et al. [16] studied the wall transport properties of a packed bed by the dissolution in water of a slightly soluble substance that coats the internal surface of the reactor tube. Both the authors adopted 2-naphthol while Dixon and co-workers also tested the use of cinnamic acid and benzoic acid in the same setup. Cadwell et al. [17] evaluated the interphase mass transfer in spinning basket reactors by dispersing pellets of naphthene in glass spheres of the same dimensions and measuring the concentration of naphthene sublimated in air or hydrogen during the operation of the reactor. Sublimation of naphthene was also employed by Breault et al. [18] as a probe in a circulating fluidized bed where a sphere of the substance was suspended by a holder in a stream of cork particles and the loss of material was evaluated during the time. The applicability of these methodologies depends on the possibility to accurately recreate the geometry to be analyzed with the soluble/sublimating material without cracks or deformations and on the stability of the sample during the measurements. For non-trivial geometries like POCS, the small dimensions involved, the impossibility of the direct 3D printing with relevant substances and the low solid fraction typical of these structures can hardly be reconciled with such an approach. Furthermore, the variable sublimation rates, which characterize the different regions of the structure (e.g. strut in crossflow versus strut intersections), determine concomitant geometrical modifications that have to be properly tracked to accurately quantify the external transport properties. As a result, such challenges make these techniques unsuitable for the evaluation of the external mass transfer coefficients in POCS.

Evaporation of a suitable liquid from an absorbent material is another technique reported in literature to evaluate the transport properties of different substrates. DeAcetis et al. [19] used spheres of celite saturated with water and mixed with plastic spheres in a packed bed reactor and measured the water vapor concentration in the flowing air. Votruba et al. [20] saturated porous honeycomb monoliths with selected liquids (water, decalin or o-xylene) and measured the rate of evaporation in a controlled air flow. The evaporation technique suffers from the problem of manufacturing POCS with a sorbent material and the limited quantity of liquid that can be held by a structure with a low solid fraction.

Catalytic reactive experiments have been extensively used in the literature for the evaluation of mass transfer properties of different catalyst supports. Bolland et al. [21] used the decomposition of O_3 catalyzed by angular cast steel particles in a circulating fluidized bed. They report that O_3 decomposition is an extremely active reaction even at low temperature and is catalyzed by a wide range of transition metal oxides [22]. However, this poses a significant problem in the design of the experimental apparatus to ensure that the sole investigated structure is active to avoid an unwanted O_3 conversion and the consequent overestimation of the mass transfer coefficients. To overcome such a limitation, the catalytic oxidation of CO over PGM (precious group metals) catalysts has been extensively employed. As reported by Ullah et al. [23] and Uberoi et al. [24], catalytic CO oxidation can be used to quantify the Sherwood numbers of ceramic and metallic monoliths. The same approach has been used by Giani et al. [25], Bracconi et al. [13] and Aguirre et al. [26] to assess external mass transfer performances of open cell foams. Catalytic-reactive tests have the advantage of preserving the shape and dimensions of the structure under analysis because the reaction takes place on the catalytic surface which remains unaltered while the consumed species are constantly replaced by the flowing fluid allowing for approaching steady state conditions. On the other hand, the necessity to reach full external mass transfer control mandates to operate at high temperatures. For CO oxidation, even on highly active catalysts, temperatures in excess of 300 °C are required to grant the complete onset of the external mass transfer regime and materials compatible with these temperatures are required for the manufacturing of the samples to be tested.

Metal-based 3D printing is a technology that, in principle, can be used for the manufacture of metallic substrates compatible with the conditions required for CO oxidation in full external mass transfer. These substrates, however, have the drawbacks of the relatively low printing quality with high rugosity of the surfaces that may impact the flow field. Moreover, the samples suffer from dimensional limitations in terms of the minimum details that can be printed. Furthermore, this technology requires long manufacturing times and highly specialized machinery needed for production and finishing with consequential high costs.

An interesting alternative for the evaluation of transport properties of novel structured supports consists in the manufacturing of resin catalyst substrates printed by stereolithography (SLA) 3D techniques, as already demonstrated by Bracconi et al. [10] for the investigation of pressure drops in open cell foams and by Lammermann et al. [14] for the analysis of pressure drops and liquid hold-up in POCS. This technology is readily available on the market at a relatively low cost. In contrast to metal selective laser sintering (SLS) or SEBM (Selective electron beam melting) machines, an SLA 3D printer is much cheaper and much easier to operate. In addition, the use of a liquid raw material ensures extremely accurate results in terms of printing quality, which is not limited by the granulometry of the starting powders.

The use of an organic resin, however, may represent a drawback of SLA 3D printing when producing samples for the evaluation of mass transfer properties. Indeed, resins have, usually, more stringent operating windows with respect to metals and ceramics in terms of ambient chemistry (i.e. they can be degraded by oxidative atmospheres) and sustainable temperatures. Such limitations can, in part, be overcome by new materials for 3D printing such as engineering resins. Among all the alternatives, resins with a high heat deformation temperature (HDT) promise a cheap alternative to metals for experimental applications that require temperatures as high as about 290 °C, thus allowing the in-house realization of samples with the geometrical accuracy needed for the evaluation of the external mass transfer properties of these geometries.

The use of a material with a maximum operating temperature of 290 °C requires, however, that the selected test reaction exhibits a fast kinetic at relatively low temperatures over supported metal catalysts. With this constraint, catalytic CO oxidation over PGM catalysts is not suitable for this purpose due to temperatures required for the complete onset of the external mass transfer regime (i.e. > 300 °C). To overcome such a limitation, catalytic oxidation of H_2 in rich conditions over PGM is herein adopted for the first time for the evaluation of mass transfer properties. Due to the extremely high activity of the reaction [27], the onset of the external mass transfer regime is obtained at significantly lower temperatures (i.e. 200 °C for H_2 oxidation versus > 300 °C for CO oxidation), thus enabling the use of the inexpensive, accurate and easily manufacturable resin samples.

In this work, we propose a novel experimental protocol for the evaluation of the external mass transfer properties of 3D printed catalyst supports. The samples are manufactured with an SLA 3D printer and a heat resistant resin at a lower price and with better accuracy than in the case of equivalent metallic 3D printed structures. The supports are, then, catalytically activated with a 3% Pd/CeO_2 washcoat deposited by spin-coating. The green active phase is then consolidated with an in-situ calcination in N_2 followed by a reduction in N_2/H_2 stream. On these samples, the gas-solid mass transfer properties are evaluated using H_2 oxidation in rich conditions. The high activity of H_2 oxidation on Pd/CeO_2 catalyst at low temperatures makes this reaction uniquely suitable for the investigation of the transport properties since full external mass transfer control is achieved at temperatures as low as 200 °C, compatible with the support resin. Moreover, the adoption of rich conditions (excess H_2) avoids the H_2 back-diffusion effects expected in the case of lean operation, enabling the assumption of a simple plug flow reactor model to compute the external mass transfer coefficient.

The protocol is first assessed by considering 3D printed replicas of

open cell foams. The mass transfer coefficients are evaluated by employing the rich H_2 oxidation and the results are compared against a well-established literature correlation for external mass transfer [13]. The herein proposed experimental methodology is general and can be directly extended to the investigation of the external mass transfer properties of structures beyond foams. In this view, 3D printed TKKD structures are also tested according to envisioned methodology to evaluate the gas-solid mass transfer properties showing the capability of the protocol to manage different structures and shape. As a further validation, the TKKD substrates are also printed in aluminium by using a metal 3D printer and the external mass transfer coefficient are evaluated using the conventional method (i.e. mass transfer limited CO oxidation over PGM-based catalyst) to confirm the equivalence of the two methodologies for the evaluation of mass transport of complex catalyst substrates.

2. Materials and methods

2.1. Resin substrate preparation

Catalyst substrate samples (digitally reconstructed open cell foams and TKKD POCS) were prepared by stereolithographic [28] 3D printing using a commercial device (Form2 printer by Formlabs). The 3D printer needs to be supplied with a file containing all the information for the correct realization of the printing layers. The first step for the definition of these files consists in the generation of the CAD files of the samples. Structure for the open cell foam samples were digitally reconstructed by imposing the cell diameter, solid fraction and circular cross-section struts with a parabolic profile as described in literature [29]. To grant that the properties extracted from the sample are representative of the structure, a minimum sample size of 3 cells, both radially and axially is needed. Due to the internal diameter of the test reactor of 9 mm, the maximum cell size that we could investigate was limited to 3 mm to meet the requirement of 3 cells in each direction.

The CAD for the TKKD POCS was generated with OpenSCAD software. The TKKD sample cell to strut diameter ratio was defined as to obtain a void fraction of 0.9 and the strut diameter was chosen as the smallest feature printable by the metallic 3D printer used for the exact replica of the samples. The cell size was chosen to have at least 3 cells in the radial direction and by considering the dimensional constraints of the metallic 3D printer (i.e. 150 μm). The sample was cut with a cylinder of the appropriate dimensions to obtain the final sample.

All the geometries were exported as STL files and imported in the PreForm software to generate the print jobs at a vertical resolution of 25 μm and with the printing profile for High Temp V1 resin.

The SLA 3D printer was loaded with high temperature resin (Formlabs FLHTAM01 High Temp V1) characterized by an $HDT_{@0.45Mpa}$ of 289 °C. Once the printing process was complete, the samples were carefully detached from the building platform of the printer and washed for 10 min in Isopropyl alcohol (IPA) to remove the uncured resin in excess. The cleaned parts were dried with compressed air to remove residual IPA and post-cured at 80 °C for at least 180 min under UV light. The supports needed for the printing process were removed from the fully hardened samples with wire cutters and the samples were polished with sandpaper to obtain clean faces.

3D printing of the metal sample was outsourced to a commercial company (AIDRO Hydraulics) due to the lack of an in-house metal printing machine. The sample was printed with a SLM machine out of an aluminum powder bed from the same. STL file used for the resin sample to obtain the same geometry within the accuracy of the 3D printing machines.

In this work, we adopt the following notation to identify the 3D printed sample: the first letter defines the geometry (F = foam, T = TKKD POCS), the first number defines the cell diameter (in mm), the second number defines the void fraction. For POCS structures: 'r' defines the resin sample and 'a' the aluminum sample.

2.2. Catalyst preparation

To catalytically activate the resin samples, Pd supported on CeO_2 was chosen as the active phase. This catalyst formulation was used in previous works using CO oxidation as the probe reaction [13], whereas the activity of Pd for the H_2 oxidation is also documented [27].

The catalyst was prepared according to a procedure previously reported in the literature [32] starting from the nitrate salts of cerium ($Ce(NO_3)_3{\cdot}6H_2O$, Sigma-Aldrich) and palladium ($Pd(NO_3)_2$ (12–16 % w/w aqueous solution from Alfa Aesar).

High surface area CeO_2 (CeHS) was prepared by precipitation with ammonium carbonate ($(NH_4)_2CO_3$, Sigma-Aldrich) [33]. A 2.6 M water solution of ammonium carbonate was added under continuous stirring to a 1 M water solution of cerium nitrate at room temperature. The resulting precipitate was filtered and washed with distilled water until a neutral pH was reached. The wet powder was dried overnight at 120 °C and the resulting powder was calcined for 3 h at 500 °C (heating and cooling rates: 2 °C/min). To catalytically activate CeHS, palladium was dispersed using the incipient wetness technique [34]. Total solution volume was calculated as the volume required to fill the CeHS pores; and the palladium nitrate concentration was calculated to reach a palladium content (Pd^0 to CeHS + palladium) of $3\%_{wt}$. The resulting powder was dried overnight at 120 °C and calcined for 10 h at 500 °C (heating and cooling rates: 2 °C/min) to decompose the palladium nitrate to palladium oxide obtaining the final catalytic powder (PdCeHS).

2.3. Washcoat deposition

According to previous findings on foams and POCS [32,35–37], spin coating was the methodology of choice for the deposition of the catalyst over the cellular samples to allow for a uniform coating of their complex geometry.

The Pd/CeO_2 slurry was prepared according to [35] by dispersing the previously described PdCeHS powder in a liquid medium composed of 1.9 w/w glycerol, 1.8 w/w distilled water and 0.07 w/w polyvinyl alcohol with respect to the powder.

The preparation consists in the dissolution of the PVA in water at 85 °C under magnetic stirring. After cooling the solution to room temperature, glycerol is added and the PdCeHS powder is mixed in in the liquid medium by ball-milling with zirconium oxide spheres for 24 h at 30 rpm. The slurry is then removed from the ball-mill and ethanol (for residue analysis, Sigma-Aldrich, 0.39 w/w with respect to the powder) is carefully added dropwise to remove the foam generated by the ball milling process.

The slurry is carefully transferred to a suitable beaker and each sample is individually dipped by hand with attention to completely submerge the support. To remove the excess formulation, samples were spun with a commercial spin-coater (SPIN 150i spinner by SPS) for 8 s @ 2500 rpm and with a speed up/down phases at 500 rpm/s. For the flash-drying, wet samples were placed in a preheated oven in air to partially consolidate the washcoat. As for the spin-coating phase, the flash-drying process is performed at conditions, namely 3 min at 200 °C in air, milder than the ones reported in literature [35] due to the nature of the support material. The conditions are sufficient to induce the evaporation of the water and glycerol, leading to samples with an almost dry washcoat while preserving the substrate from thermal degradation. After flash-drying, the samples are cooled to room temperature and the amount of deposited washcoat is evaluated by gravimetric analysis.

The deposition/flash-drying procedure was repeated up to 3 times to reach a minimum target catalyst loading, (7 g_{cat}/l) calculated as the deposited mass divided by the total volume of the sample (solid plus empty fraction). Calcination at 500 °C for 10 h (2 °C min^{-1} heating and cooling ramps) was performed only for the aluminum sample due to the inability of the resin to withstand the temperature required by the process.

Foam samples were activated for the entire length whereas TKKD

samples were coated only for the last 9 mm (4.5 cell diameters) to avoid on one side flow maldistributions and on the other hand excessive conversion during the reactive tests.

Due to the impossibility to perform a calcination treatment on the resin samples as described in the reference procedure [35], a two-steps, in-situ, activation procedure was performed in order to stabilize and activate the catalytic washcoat. During the first step, after loading the sample in the reaction tube, the sample was heated to 260 °C at a rate of 2 °C/min in a flow 0.75 Nl/min of N_2 and is kept at the target temperature for 6 h. The sample was, then, cooled to room temperature in N_2 atmosphere. During the second step, the sample was subjected to a reduction treatment in a flow of 2.5 % H_2 in N_2 at 0.75 Nl/min where it is heated to 260 °C at a rate of 2 °C/min, hold 6 h and cooled to room temperature. After the end of the thermal treatment, the sample was recovered and visually inspected to verify the absence of damages. Finally, the reactor was cleaned to remove any residue of the powder catalyst before being reloaded with the sample to be tested.

Coating homogeneity was verified with the aid of an optical microscope (SteREO Discovery.V12 with Axiocam ERc 5 s camera, Zeiss).

2.4. Catalytic tests

External mass transfer rates for the different structured supports were evaluated by running H_2 oxidation (Eq. 1) tests in rich conditions.

$$H_2 + \tfrac{1}{2}O_2 \rightarrow H_2O \quad (1)$$

The reaction was performed in excess of H_2 in order to keep conversion limited by the O_2 diffusional rate. Based on the considerations reported in the Supplementary Material (S1), H_2 rich combustion tests were performed with a feed stream containing 4% H_2, 1% O_2 and 95 % N_2 v/v at flowrates between 3 and 9 Nl/min with step increments of 1 Nl/min. This choice was dictated by the different diffusion coefficients of O_2 and H_2. H_2 diffusivity is about five times greater than O_2 diffusivity, which makes the collection of mass transfer controlled conversion data far enough from 100 % only possible at extremely high gas velocities. Besides lean H_2 combustion result in over adiabatic temperatures at the catalyst surface, which can exceed the resin stability limit.

To perform a direct comparison between the proposed methodology and CO oxidation (Eq. 2) in the external mass transfer control, 1.5 % CO in air was used as the feed mixture at flowrates between 3 and 9 Nl/min as reported in [13].

$$CO + \tfrac{1}{2}O_2 \rightarrow CO_2 \quad (2)$$

The catalytic tests were run in a 9 mm ID reactor tube heated by an external electric oven as reported in Fig. 1.

To monitor the temperature of the catalyst, two thermocouples were placed immediately before and after the sample and the arithmetic mean of T_{in} and T_{out} was considered as the representative temperature for the evaluation of the transport properties. The temperature difference between the two thermocouples caused by the exothermicity of the reaction was lower than 70 °C.

Three independent mass flow controllers (5850E model by Brooks) were used to regulate the flows of N_2, H_2 or CO and air. The gas streams were mixed in a single line and fed to the reactor where they were preheated and contacted with the structured catalyst sample. To analyze the composition of the gas mixture, a micro-GC (GCX from Pollution) was used. H_2 (or CO when used instead), O_2 and N_2 were separated in a capillary column coated with 5 Å molecular sieves, using Ar as carrier and as reference gas for the thermal conductivity detector (TCD). Gas composition was calculated using N_2 as internal standard and H_2O was inferred from the conversion of H_2. A bypass line (normally closed) was installed to allow for the analysis of the feed gas in order to calculate the effective conversions.

Due to the inability to track the production of water, the following criterion for the mass balances based on the stoichiometry of molar consumptions of O_2 and H_2 is introduced (Eq. 3).

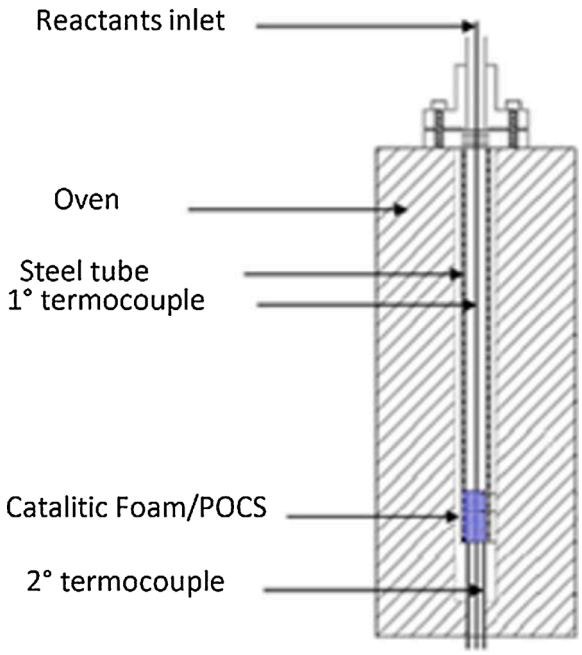

Fig. 1. Sketch of the reactor configuration.

$$Err_{H_2} = 1 - \frac{H_2^{in} - H_2^{out}}{2\cdot\left(O_2^{in} - O_2^{out}\right)} \quad (3)$$

where H_2^{in} and O_2^{in} are the molar flow rates fed to the reactor and H_2^{out} and O_2^{out} are the outlet molar flow rates measured after the reaction section. The measurement was considered acceptable when the error was less than 5%.

For the aluminum POCS sample, the analysis of CO_2 was performed through a capillary column coated with Porapack Q with He serving both as reference and carrier gas.

To calculate accurately the CO conversion, CO_2 production was monitored, and the conversions were considered reliable with an error in the carbon balance lower than 5% as per to Eq. 4.

$$Err_{CO} = 1 - \frac{CO^{out} + CO_2^{out}}{CO^{in}} \quad (4)$$

The analysis of conversion data in full external mass transfer regime was performed with the classical approach of dimensionless numbers. For the H_2 oxidation runs, conversions were evaluated directly from the consumed oxygen (Eq. 1) while, in the case of CO oxidation, CO_2 production was used to infer the CO conversion according to the stoichiometry of the reaction (Eq. 2).

To analyze the transport properties of the different samples, the estimates of the mass transfer coefficient k_m, were calculated for each flowrate according to Eq. 5 by assuming full external mass transfer control in an ideal plug flow reactor (PFR) [13]

$$k_m = \frac{-\ln(1-\chi)\cdot u}{S_v \cdot l} \quad (5)$$

where χ is the conversion, u is the superficial gas velocity calculated at the bed average operating temperature and pressure, S_v is the specific surface area and l is the catalytically active length.

For the dimensionless analysis, the characteristic length (l_{car}) is the averaged strut diameter for open cell foams (as proposed in [13] and [30]) and the strut diameter for TKKD. Sherwood and Reynolds numbers were therefore calculated according to Eq.s 6–8:

$$Sh = \frac{k_m D_{lim}}{l_{car}} \quad (6)$$

$$Re = \frac{\rho u l_{car}}{\mu} \quad (7)$$

$$Sc = \frac{\mu}{\rho D_{lim}} \quad (8)$$

where μ is the viscosity of the gas mixture, ρ the density, and D_{lim} the diffusivity of the limiting reactant, O_2 and CO in the different experiments, respectively.

3. Results and discussion

3.1. 3D printing

The quality of the printed sample was verified by comparing the measured solid fraction with the design one. To calculate the void fraction (ε), the samples were individually weighted, and their external dimensions were measured with the aid of a caliper:

$$\varepsilon = 1 - \frac{w_{sample}}{\rho_{mat} \cdot V_{tot}} \quad (9)$$

where w_{sample} is the sample weight and V_{tot} is the sample volume and ρ_{mat} is the density of the printing material (i.e. resin or aluminum alloy).

The density of the resin was evaluated from a dense cube printed with the same printing parameters as the POCS samples (ρ_{mat}= 1.23 g/cm^3). In the case of the aluminum POCS, the bulk density of the material was assumed equal to that of the aluminum alloy powder (AlSi10) used as the raw material (ρ_{mat} = 2.65 g/cm^3).

The strut diameter and the cell size were also measured with the aid of optical microscopy to understand possible printing deviations.

A good agreement between the 3D printed and CAD structures was obtained, since the deviation between the experimental and the theoretical (*design*) void fraction was less than ±1% for the ε = 0.9 structures and 2% for the ε = 0.8 foam, as reported in Table 1.

Fig. 2 shows the 3D printed foam samples as well as the TKKD structures both in resin and aluminum (i.e. samples T_20−0.90 r and T_20−0.90a, respectively). As clearly visible, the surface finish of the resin substrates is significantly smoother than the one at of the metallic structure.

3.2. Characterization of the coating

The use of supports in polymeric resin leads to the necessity of tailoring the coating procedure to the properties of the resin. In particular, for the deposition of the catalytic layers, spin coating speed and duration were reduced with respect to the parameters used in previous work [35] to cope with the reduced adhesion offered by the resin to the slurry.

3.2.1. Thermogravimetric analysis

Before performing the coating deposition, thermal stability of the resin was assessed to define the temperature range at which the flash drying cycles can be performed without causing the degradation of the resin. For this reason, a drop of slurry, as well as two fragments of the printed resin supports (~ 5 mg each, bare and coated with wet slurry) were tested by thermogravimetric (TG) analyses.

As shown by the TG analysis performed on the wet slurry (Fig. 3a), the liquid components of the formulation start evaporating between 50 and 100 °C and are completely removed at 250 °C with no significant differences between the analysis in N_2 and air, indicating that the combustion of the organic fraction is not involved. Fig. 3b shows that the resin is stable up to 290 °C where the first weight loss is observed. Between 400 °C and 450 °C the resin undergoes significant degradation while oxidation seems to occur between 450 °C and 600 °C as shown by the different trend between the tests performed in N_2 and Air.

By performing a TG analysis on the slurry/resin combination (Fig. 3c), the temperature at which the coating is completely dried is reduced to 200 °C while resin degradation is not significant for temperature below 290−300 °C, suggesting the absence of catalytic effects of the coating on the degradation of the resin.

Nevertheless, flash drying at 250 °C leads to the occasional degradation of the resin samples. A possible explanation for this phenomenon can be traced to the severity of the temperature change and the exothermicity of the decomposition of the organics in the slurry that further increases the local temperature and starts the decomposition of the material. In view of this, a temperature of 200 °C was chosen for the flash drying.

3.3. Washcoat deposition

All samples were washcoated with a single deposition step resulting in a specific loading of around 10 g/l with the exception of the aluminum POCS (23.6 g/l).

The actual specific load (*Sl*) was determined by weight differences of the samples after each spin-coating / flash-drying cycle from the bare ones, m_W (Eq. 10)

$$Sl\ [g/l] = m_W / V_{coat} \quad (10)$$

where the coated volume (V_{coat}) corresponds to the whole sample in the case of foam replicas or a sample fraction in the case of TKKD samples (POCS were coated only for half the total length to reduce the total conversion while maintaining a representative fluid-dynamic behavior [13]).

The washcoat thickness ($t_{w,avg}$) was estimated from the specific load (*Sl*) for each sample according to Eq. 11:

$$t_{w,avg} = \frac{Sl}{\rho_{coat} \cdot Sv} \quad (11)$$

The coating density (ρ_{coat}) is assumed to be 2.0 g/cm^3 [32] and the

Table 1
Measured void fractions and geometrical characteristics of the tested samples.

Sample	Cell diameter Average [mm]	Strut diameter Average [μm]	Void fraction [-]	Specific surface area [m^{-1}]	Diameter [mm]	Length [mm]
F_2.5−0.90	2.51 *(2.50)*	305 *(314)*	0.905 *(0.90)*	895 *(916)*	9	14.5
F_3.0−0.80	2.98 *(3.00)*	652 *(617)*	0.783 *(0.80)*	947 *(935)*	9	13.7
F_3.0−0.90	3.01 *(3.00)*	357 *(377)*	0.908 *(0.90)*	738 *(763)*	9	16.0
T_2.0−0.90 r	2.00 *(2.00)*	247 *(259)*	0.913 *(0.90)*	1305 *(1352)*	9	18.5
T_2.0−0.90a	1.99 *(2.00)*	269 *(259)*	0.898 *(0.90)*	1388 *(1352)*	9	20.0

() design values are reported in parenthesis.

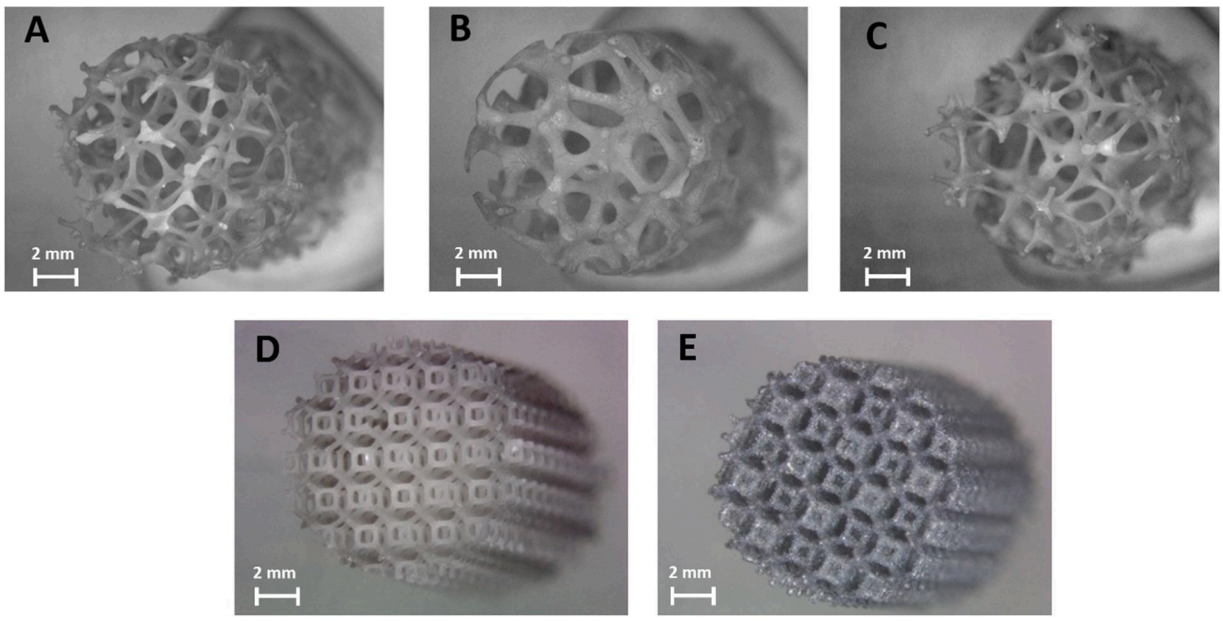

Fig. 2. Optical microscope images of 3D printed support samples for foams: A) F_2.5-0.90, B) F_3.0-0.80, C) F_3.0-0.90 and POCS: D) T_2.0-0.90 r, E) T_2.0-0.90a.

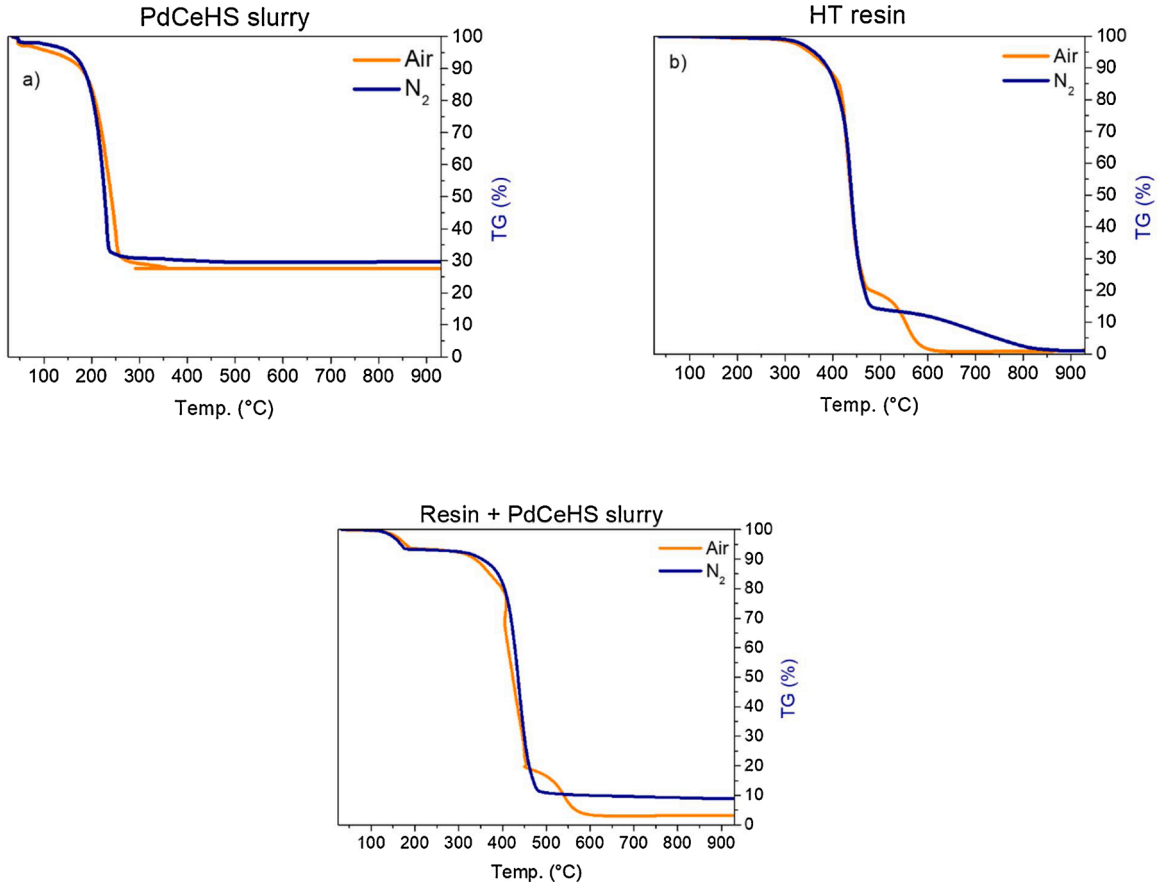

Fig. 3. TGA results of a) Pd/CeO_2 wet slurry, b) HT resin, c) HT resin coated with Pd/CeO_2 slurry.

sample volume and specific surface areas are reported in Table 1.

As observed in previous studies [32], the total amount of deposited catalyst on the printed foam samples depends almost linearly on the specific surface area (see Table 2), since the washcoat thickness is controlled mainly by the slurry rheology and spin coating velocity, resulting in a constant thickness of about 5.5 μm.

For the tetrakaidecahedron POCS, a catalyst load of 4.9 mg was obtained in a single step on the resin sample, while for the aluminum sample a higher load of 13.5 mg was achieved after just one coating step corresponding to a washcoat thickness of 8.5 μm, likely due to the surface roughness which increases the wet coating adhesion.

The washcoat layers deposited on all the samples appeared to be

Table 2
Geometrical properties of the structures after the coating.

Sample	Measured load [mg]	Washcoat thickness [μm]	Specific load [g/l]	S_v washcoated [m^{-1}]	Washcoated length [mm]	Strut diameter washcoated [μm]	Void fraction washcoated [-]
F_2.5−0.90	9.3	5.63	9.94	923	14.5	319	0.900
F_3.0−0.80	10.5	6.29	12.5	950	13.7	656	0.777
F_3.0−0.90	7.1	4.73	6.98	763	16.0	377	0.905
T_2.0−0.90a	13.5	8.49	23.6	1417	9.0	276	0.886
T_2.0−0.90 r	4.9	3.47	9.06	1527	8.5	309	0.911

homogeneous and neither uncoated spots nor closed pores were found, as shown in Fig. 4.

3.4. Catalytic tests

Catalytic tests were performed at flowrates between 3 Nl/min and 9 Nl/min with increments of 1 Nl/min: in each test the temperature was increased stepwise until external mass transfer was reached.

3.4.1. Light-off curve

A metallic (Aluminum) 3D printed sample and an identical replica 3D printed in HT resin (T_2.0−0.90, Table 2), both activated with 3% Pd/CeO_2 according to the procedure reported in Section 2.3, were tested in CO oxidation and H_2 oxidation, respectively, at temperatures sufficient for the onset of full external mass transfer control. The light-off curves of H_2 oxidation and CO oxidation at 6 Nl/min are reported in Fig. 5.

At temperatures below 250 °C, the CO oxidation curve shows a low conversion with a strong dependence on temperature, suggesting that the reaction rate is mainly controlled by kinetics. At temperatures higher than 300 °C, the temperature dependence of conversion is significantly reduced, consistently with the onset of external mass transfer limitations. The temperature required for the onset of full external mass transfer control is clearly not compatible with the use of resin supports ($T_{max} = 290$ °C, Fig. 3). Conversely, H_2 oxidation reveals a high catalytic activity already at 100 °C. Above 180 °C, oxygen conversion shows a quasi-negligible temperature dependence, and the full external mass transfer control is reached for temperatures higher than 200 °C.

It is important noticing that, while both sets of data were extracted from runs at the same specific flowrate (i.e. 6 Nl/min) on the same geometry (TKKD_2.0−0.9), the difference in external mass transfer limited conversion is related to the intrinsic differences of the samples (coated

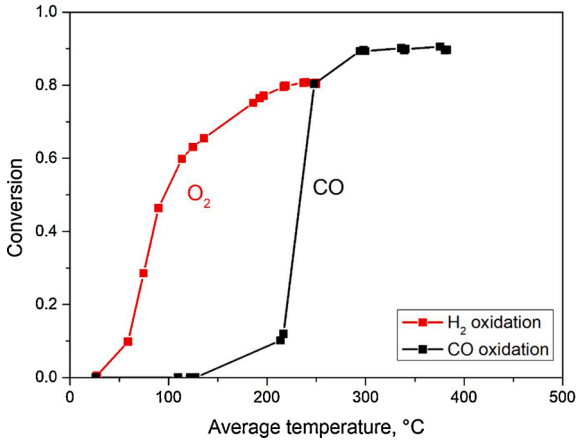

Fig. 5. Light off curves for H_2 oxidation over sample T_2.0-0.9 r and CO oxidation over sample T_2.0-0.9a. Conversions of O_2 and CO respectively.

length for resin sample equal to 8.5 mm vs aluminum sample equal to 9 mm and small deviations in the geometry due to different catalyst loading, see Table 2). For this reason, the extrapolation of the external mass transfer coefficients is needed to reconciliate the results

3.4.2. Catalyst stability

To assess the stability of the coating after the thermal treatment, tests at 3, 6 and 9 Nl/min were repeated in succession three times on a new sample to verify the stability of the washcoat and the reproducibility of the obtained data.

As shown in Fig. 6 (open symbols), data gathered during the reproducibility tests are comparable to the values obtained during the first

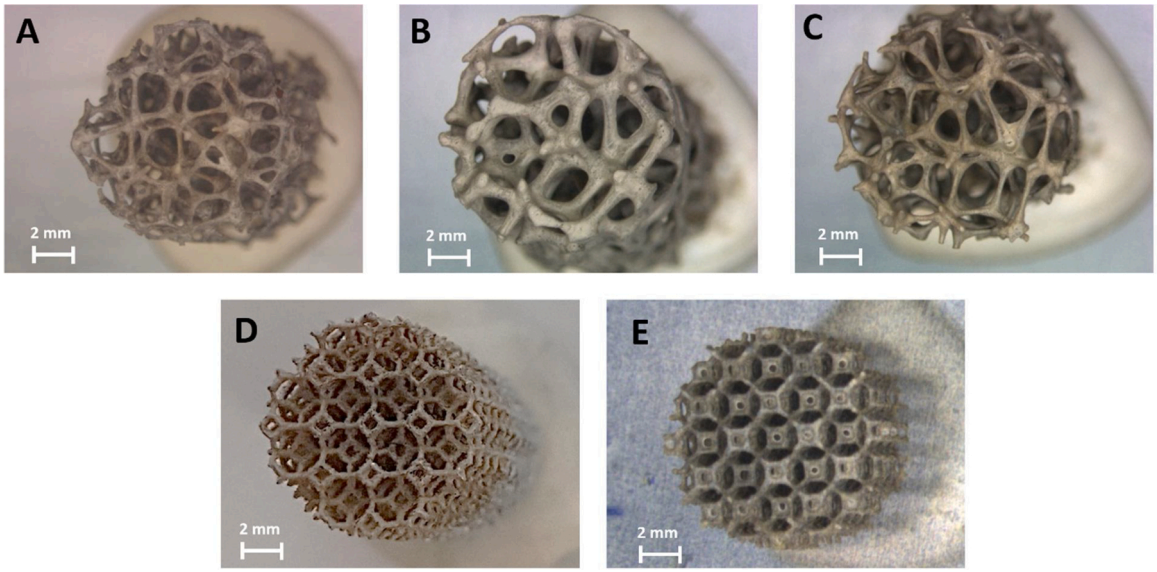

Fig. 4. Optical microscope images of washcoated support samples for foams: A) F_2.5-0, B) F_3.0-0.80, C) F_3.0-0.90 and POCS: D) T_2.0-0.90a, E) T_2.0-0.90 r.

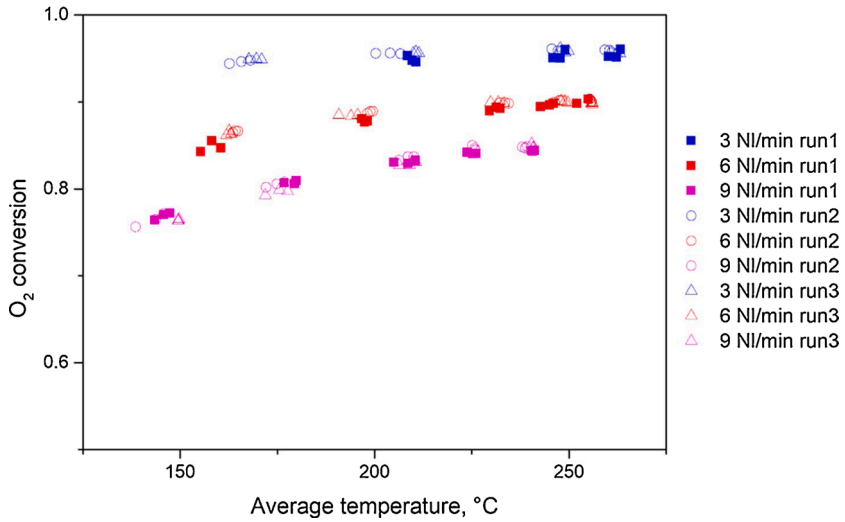

Fig. 6. O_2 conversion with respect to the average temperature for reproducibility runs (full symbols corresponds to run 1, open circles to run 2 and open triangles to run 3). Runs are reported in chronological order in the legend.

run (solid symbols).

The repeated tests performed on these resin supports thus suggest that the deposition and activation protocols herein developed result in washcoat layers stable enough at the conditions required by the experimental protocol to guarantee the reproducibility of the results.

3.5. Evaluation of mass transfer properties

3.5.1. Foam replicas

The dimensionless mass transfer coefficients estimated by testing of 3D printed foam resin replicas were compared with the Sherwood correlation derived by Bracconi et al. [13].

Excellent agreement with very limited deviation (i.e. < 7 %) is observed between the literature correlation (whose applicability is for $1 < Re_{ds} < 300$, $0.7 < \varepsilon < 0.95$ and $0.3\ mm < d_c < 5\ mm$ with deviations below ±15 %) and the experimental data for the foam samples, regardless of the different cell diameter and void fractions (Fig. 7). Deviations from the correlation at low Reynolds numbers can be recognized for one of the tested supports, namely the foam F_2.5−0.9, at low Re (i.e. < 20). This can be ascribed to the very high conversions (i.e. > 93 %) obtained at such conditions which may result in a magnification of the experimental error. Regardless of the wider uncertainty at high conversion values, all data points are within the ±15 % validity range of the literature correlation [13].

These results, coupled with the direct comparison against literature established CO oxidation reactive tests, suggest that the hereby proposed methodology enables the accurate evaluation of external mass transfer coefficients of complex 3D geometries with a high degree of accuracy and reliability.

3.5.2. TKKD POCS

A direct comparison between the newly proposed methodology and the conventional CO oxidation-based approach in the external transport limited regime was performed on samples T_2.0−0.9a and T_2.0−0.9 r.

To compensate for both the differences in the samples geometry (i.e. resin sample active length equal to 8.5 mm vs. aluminum sample equal to 9 mm and small geometrical deviations as listed in Table 2) and average temperature, a comparison in terms of Sherwood numbers is required and is used below to assess the mass transfer behavior of the two systems (Fig. 8).

Fig. 8 compares the dimensionless mass transfer coefficients for CO oxidation over the aluminum sample and for H_2 rich oxidation over the resin sample. Error bars are calculated by assuming a 2% uncertainty on the conversion values based on the standard deviation estimated from

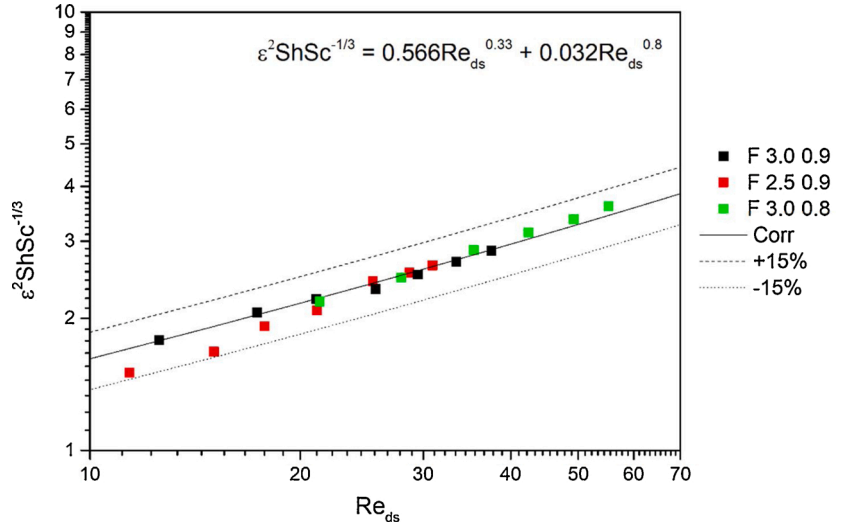

Fig. 7. Comparison between literature correlation for open cell foams mass transfer and experimental results [13].

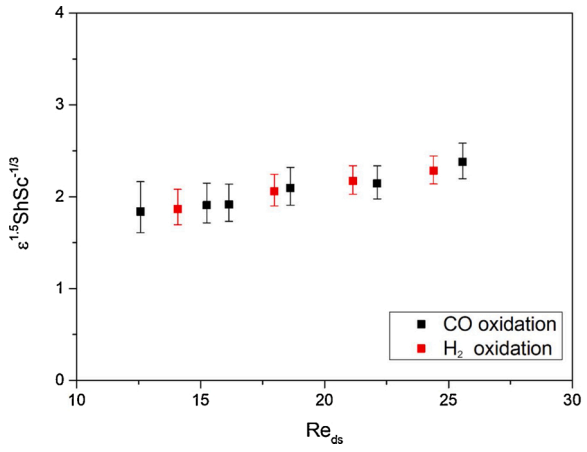

Fig. 8. $\varepsilon^{1.5}Sh/Sc^{1/3}$ vs Re comparison between H_2 oxidation with resin support and CO oxidation with aluminium support for the T_2.0-0.9 sample.

the reproducibility runs.

The void fraction of the samples shows small differences (0.886 for the aluminum sample vs 0.911 for the resin one) due to the manufacturing and coating procedures. Therefore, a possible influence of the porosity on the Sh numbers could hinder the comparison between the two methodologies. To overcome such a limitation, we introduced a dependence on the void fraction equal to $\varepsilon^{1.5}$, as suggested by Ferroni et al. [38], to remove any additional dependence on the geometrical properties.

An excellent agreement between the two dataset is observed, as shown in Fig. 9, proving the total equivalence of the two methodologies.

4. Conclusions

A new inexpensive, fast and highly accurate experimental protocol has been developed for the evaluation of external/interphase mass transfer properties of cellular structured catalyst supports. This protocol relies on the 3D printing (SLA) of an HT resin to manufacture samples with better accuracy than metal printed structures. These resin supports are, subsequently, catalytically activated towards rich H_2 oxidation by performing the deposition of a Pd/CeO_2 washcoat by spin-coating followed by a two-step, in-situ calcination / reduction protocol with N_2/H_2. The washcoated samples were finally tested in rich H_2 oxidation under full external mass transfer control. The method was first validated for open cell foams replicas by successfully comparing the results with previously derived correlations, which resulted in excellent agreement. Moreover, a direct comparison was performed between a resin TKKD structure and a metallic (Al) sample printed from the same CAD file. These samples were tested according to the herein proposed methodology and using the conventional CO oxidation approach, respectively: the results of the two campaigns were essentially superimposed, thus validating the novel approach herein presented.

This work provides the basis for the application of this method to the experimental investigation of mass transfer properties of a wide range of structures. The possibility to print substrates with a fast and economical lab-scale printer and test them extensively using the peculiar characteristics of rich H_2 oxidation to recover Sherwood-Reynolds correlations can be coupled, as previously demonstrated [10], with the investigation of pressure drops to fully characterize the fluid dynamic and transport properties of novel geometries for cellular catalyst substrates. The application of resin-based 3D printed samples for mass transfer studies is reported here for the first time.

CRediT authorship contribution statement

Federico Sascha Franchi: Data curation, Methodology, Investigation, Validation, Formal analysis, Visualization, Writing - original draft. **Matteo Ambrosetti:** Methodology, Investigation, Validation, Formal analysis, Conceptualization, Writing - original draft. **Riccardo Balzarotti:** Methodology, Investigation, Conceptualization, Writing - original draft. **Mauro Bracconi:** Methodology, Conceptualization, Writing - original draft. **Gianpiero Groppi:** Conceptualization, Methodology, Resources, Writing - review & editing, Supervision. **Enrico Tronconi:** Conceptualization, Resources, Writing - review & editing, Supervision, Project administration, Funding acquisition.

Declaration of Competing Interest

The authors declare that they have no known competing financial interests or personal relationships that could have appeared to influence the work reported in this paper.

Acknowledgments

The research leading to these results has received funding from the European Research Council under the European Union's Horizon 2020 Research and Innovation Program (Grant Agreement no. 694910/ INTENT: "Structured Reactors with Intensified Energy Transfer for Breakthrough Catalytic Technologies") and from MIUR, FARE RICERCA IN ITALIA, project BEATRICS Grant R16R7NLWPW.

Appendix A. Supplementary data

Supplementary material related to this article can be found, in the online version, at doi:https://doi.org/10.1016/j.cattod.2021.04.004.

References

[1] A. Cybulski, A.J. Moulijn, Structured Catalysts and Reactors, second ed., CRC Press, 2005 https://doi.org/10.1201/9781420028003.
[2] L. Giani, G. Groppi, E. Tronconi, Mass-transfer characterization of metallic foams as supports for structured catalysts, Ind. Eng. Chem. Res. 44 (2005) 4993–5002, https://doi.org/10.1021/ie0490886.
[3] L. Fratalocchi, G. Groppi, C.G. Visconti, L. Lietti, E. Tronconi, Adoption of 3D printed highly conductive periodic open cellular structures as an effective solution to enhance the heat transfer performances of compact fischer-tropsch fixed-bed reactors, Chem. Eng. J. 386 (2020), https://doi.org/10.1016/j.cej.2019.123988.
[4] R. Balzarotti, M. Ambrosetti, A. Beretta, G. Groppi, E. Tronconi, Investigation of packed conductive foams as a novel reactor configuration for methane steam reforming, Chem. Eng. J. 391 (2020), https://doi.org/10.1016/j.cej.2019.123494.
[5] C. Busse, H. Freund, W. Swieger, Intensification of heat transfer in catalytic reactors by additively manufactured periodic open cellular structures (POCS), Chem. Eng. Process. 126 (2018) 178–189, https://doi.org/10.1016/j.cep.2018.02.027.
[6] K. Boomsma, D. Poulikakos, F. Zwick, Metal foams as compact high performance heat exchangers, Mech. Mater. 35 (2003) 1161–1176, https://doi.org/10.1016/j.mechmat.2003.02.001.
[7] B. Schimmoeller, H. Schulz, S.E. Pratsinis, A. Bareiss, A. Reitzmann, B. Kraushaar-Czarnetzki, Ceramic foams directly-coated with flame-made V2O5/TiO2 for synthesis of phthalic anhydride, J. Catal. 243 (2006) 82–92, https://doi.org/10.1016/j.jcat.2006.07.007.
[8] F.C. Patcas, The methanol-to-olefins conversion over zeolite-coated ceramic foams, J. Catal. 231 (2005) 194–200, https://doi.org/10.1016/j.jcat.2005.01.016.
[9] M. Klumpp, A. Inayat, J. Schwerdtfeger, C. Korner, R.F. Singer, H. Freund, W. Schwieger, Periodic open cellular structures with ideal cubic cell geometry: effect of porosity and cell orientation on pressure drop behavior, Chem. Eng. J. 242 (2014) 364–378, https://doi.org/10.1016/j.cej.2013.12.060.
[10] M. Bracconi, M. Ambrosetti, O. Okafor, V. Sans, X. Zhang, X. Ou, C. Pereira Da Fonte, X. Fan, M. Maestri, G. Groppi, E. Tronconi, Investigation of pressure drop in 3D replicated open-cell foams: coupling CFD with experimental data on additively manufactured foams, Chem. Eng. J. 377 (2019) 120–123, https://doi.org/10.1016/j.cej.2018.10.060.
[11] N. Gargiulo, D. Caputo, G. Totarella, L. Lisi, S. Cimino, Me-ZSM-5 monolith foams for the NH3-SCR of NO, Catal. Today 304 (2018) 112–118, https://doi.org/10.1016/j.cattod.2017.10.024.
[12] N.F.B. Rebelo, K.A. Andreassen, L.I.S. Ríos, J.C.P. Camblor, H. Zander, C. A. Grande, Pressure drop and heat transfer properties of cubic iso-reticular foams, Chem. Eng. Process. 127 (2018) 36–42, https://doi.org/10.1016/j.cep.2018.03.008.
[13] M. Bracconi, M. Ambrosetti, M. Maestri, G. Groppi, E. Tronconi, A fundamental investigation of gas/solid mass transfer in open-cell foams using a combined

experimental and CFD approach, Chem. Eng. J. 352 (2018) 558–571, https://doi.org/10.1016/j.cej.2018.07.023.
[14] M. Lammermann, G. Horak, W. Schwieger, H. Feund, Periodic open cellular structures (POCS) for intensification of multiphasereactors: liquid holdup and two-phase pressure drop, Chem. Eng. Process. 126 (2018) 178–189, https://doi.org/10.1016/j.cep.2018.02.027.
[15] S. Yagi, N. Wakao, Heat and mass transfer from wall to fluid in packed beds, AIChE 5 (1959) 79–85, https://doi.org/10.1002/aic.690050118.
[16] A.G. Dixon, M. DiCostanzo, B.A. Soucy, Fluid-phase radial transport in packed beds of low tube-to-particle diameter ratio, Int J. Heat Mass Trans. 27 (1984) 1701–1713, https://doi.org/10.1016/0017-9310(84)90153-4.
[17] L. Cadwell, Gas-solid mass transfer in a spinning catalyst basket reactor, Appl. Catal. 4 (1982) 13–18, https://doi.org/10.1016/0166-9834(82)80284-4.
[18] C.P. Guenther, R.W. Breault, Mass transfer in core-annular and fast fluidization flow regimes of a CFB, Powder Technol. 190 (2009) 385–389, https://doi.org/10.1016/j.powtec.2008.08.021.
[19] J. DeAcetis, G. Thodos, Mass and heat transfer in flow of gases through spherical packings, Ind. Eng. Chem. 52 (1960) 1003–1006, https://doi.org/10.1021/ie50612a026.
[20] J. Votruba, O. Mikuš, K. Nguen, V. Hlaváček, V. Skřivánek, Heat and mass transfer in honeycomb catalysts-II, Chem. Eng. Sci. 30 (1975) 201–206, https://doi.org/10.1016/0009-2509(75)80006-6.
[21] O. Bolland, R. Nicolai, Describing mass transfer in circulating fluidized beds by ozone decomposition, Chem. Eng. Comm 187 (2001) 1–21, https://doi.org/10.1080/00986440108912877.
[22] C. Heisig, W. Zhang, S.T. Oyama, Decomposition of ozone using carbon-supported metal oxide catalysts, Appl. Catal. B-Environ 14 (1997) 117–129, https://doi.org/10.1016/S0926-3373(97)00017-9.
[23] U. Ullah, S.P. Waldram, T. Truex, C.J. Bennett, Monolithic reactors: mass transfer mesurements under reacting conditions, Chem. Eng. Sci. 47 (1992) 2413–2418, https://doi.org/10.1016/0009-2509(92)87069-3.
[24] M. Uberoi, C.J. Pereira, External mass transfer coefficients for monolith catalysts, Ind. Eng. Chem. Res. 35 (1996) 113–116, https://doi.org/10.1021/ie9501790.
[25] L. Giani, G. Groppi, E. Tronconi, Mass transfer characterization of metallic foams as supports for structured catalysts, Ind. Eng. Chem. Res. 44 (2005) 4993–5002, https://doi.org/10.1021/ie0490886.
[26] A. Aguirre, V. Chandra, E.A.J.F. Peters, J.A.M. Kuipers, M.F. Neira D'Angelo, Open-cell foams as catalysts supports: a systematic analysis of the mass transfer limitations, Chem. Eng. J. 393 (2020), https://doi.org/10.1016/j.cej.2020.124656.
[27] M. Haruta, H. Sano, Catalytic combustion of hydrogen I - its role in hydrogen utilization system and screening of catalyst materials, Int. J. Hydrog. Eenrgy 6 (1981) 601–608, https://doi.org/10.1016/0360-3199(81)90025-2.
[28] C. Parra-Cabrera, C. Achille, S. Kuhn, R. Ameloot, 3D printing in chemical engineering and catalytic technology: structured catalysts, mixers and reactors, Chem. Soc. Rev. 47 (2017), https://doi.org/10.1039/C7CS00631D.
[29] M. Bracconi, M. Ambrosetti, M. Maestri, G. Groppi, E. Tronconi, A systematic procedure for the virtual reconstruction of open-cell foams, Chem. Eng. J. 315 (2017) 608–620, https://doi.org/10.1016/j.cej.2017.01.069.
[30] M. Ambrosetti, M. Bracconi, G. Groppi, E. Tronconi, Analytical geometrical model of open cell foams with detailed description of strut-node intersection, Chem. Ing. Tech. 89 (2017) 915–925, https://doi.org/10.1002/cite.201600173.
[32] M. Ambrosetti, R. Balzarotti, C. Cristiani, G. Groppi, E. Tronconi, The influence of the washcoat deposition process on high pore density open cell foams activation for CO catalytic combustion, Catalysts 8 (2018) 510, https://doi.org/10.3390/catal8110510.
[33] R. Balzarotti, C. Italiano, L. Pino, C. Cristiani, A. Vita, Ni/CeO_2-thin ceramic layer depositions on ceramic monoliths for syngas production by oxy steam reforming of biogas, Fuel Process. Technol. 149 (2016) 40–48, https://doi.org/10.1016/j.fuproc.2016.04.002.
[34] A. Montebelli, C.G. Visconti, G. Groppi, E. Tronconi, C. Cristiani, C. Ferreira, S. Kohler, Methods for the catalytic activation of metallic structured substrates, Catal. Sci. Technol. 4 (2014) 2846–2870, https://doi.org/10.1039/c4cy00179f.
[35] R. Balzarotti, C. Cristiani, S. Latorrata, A. Migliavacca, Washcoating of low surface area cerium oxide on complex geometry substrates, Part. Sci. Technol. 34 (2016) 184–193, https://doi.org/10.1080/02726351.2015.1058872.
[36] P.H. Ho, M. Ambrosetti, G. Groppi, E. Tronconi, J. Jaroszewicz, F. Ospitali, E. Rodríguez-Castellón, G. Fornasari, A. Vaccari, P. Benito, One-step electrodeposition of Pd–CeO2 on high pore density foams for environmental catalytic processes, Catal. Sci. Technol. 8 (2018) 4678–4689, https://doi.org/10.1039/C8CY01388H.
[37] P.H. Ho, M. Ambrosetti, G. Groppi, E. Tronconi, G. Fornasari, A. Vaccari, P. Benito, Electrodeposition of CeO2 and Pd-CeO2 on small pore size metallic foams: selection of deposition parameters, Catal. Today 334 (2019) 37–47, https://doi.org/10.1016/j.cattod.2019.02.005.
[38] C. Ferroni, M. Bracconi, M. Ambrosetti, M. Maestri, G. Groppi, E. Tronconi, A Fundamental Investigation of gas/solid Heat and Mass Transfer in Structured Catalysts Based on Periodic Open Cellular Structures (POCS), submitted to Industrial & Engineering Chemistry Research, 2021.